Structure and Stability of Br_4 and Br_4^{2-} and Their Interaction with Cations and Transition Metals

Santiago Alvarez,*† Fernando Mota,‡ and Juan Novoa‡

Contribution from the Departament de Química Inorgànica and the Departament de Química Física, Universitat de Barcelona, 08028 Barcelona, Spain. *Received January 6, 1987*

Abstract: A theoretical study of the intrinsic stability of the tetrahalogen species X_4^{n-} (n = 0, 1, 2) and the effect of their interaction with alkali metal cations or with transition-metal fragments has been carried out. Extended-Hückel as well as pseudopotential ab initio calculations on these species, mostly for X = Br, have been carried out. The neutral Br_4 species is stable toward dissociation and can be described as two weakly interacting Br_2 molecules. Symmetry arguments indicate that an angular geometry is more stable than a linear one for this species. Unlike the free molecule, a bridging Br_4 ligand in a dinuclear transition-metal complex is more stable in its linear conformation; the M–Br_4–M skeleton, however, is expected to be bent according to the orbital analysis presented here. On the other hand, Br_4^- and Br_4^{2-} are both linear, but while Br_4^- is stable toward dissociation into Br_3^- and $Br^\bullet$, Br_4^{2-} dissociates without barrier, giving Br_3^- and Br^-. The interaction of Br_4^{2-} with alkali metal cations is found to have a marked directional character and is stabilizing. Coordination to transition-metal fragments is even more effective in stabilizing this anion. In contrast with the neutral species, the central bond of Br_4^{2-} is stronger than the terminal ones, in excellent agreement with the experimental bond distances found in analogous I_4^{2-} complexes.

The existence of polyhalide ions X_n^{m-} with n odd has been known for many years and is well documented,[1] but much less is known about even species such as X_4^{2-}. Neutral X_4 species have been detected spectroscopically as self-associated X_2 molecules,[2] while X_4^- ions have been only detected by ESR for X = I upon γ irradiation of I_2.[3] A salt of formula CsI_4 has been structurally characterized and found to be formed by I_8^{2-} ions.[4] However, X_4^{2-} ions have been reported in a few chain structures: Br_4^{2-} acts as a bridging ligand between $Cu(NH_3)_4^{2+}$, $Pt(phen)I_2^{2+}$, or $\{Ir(Cp)I\}_2$ groups.[6-8] I_4^{2-} ions are also present in $Tl_6Ag_2I_{10}$ and Tl_6PbI_{10}, occupying channels in the solid.[9]

The purpose of the present work is to study the electronic structure of such polyhalogen species, notably their intrinsic stability and the effect of the interaction with a cationic sublattice or with a transition metal. Although the present study is qualitative, pseudopotential ab initio calculations have been carried out on the isolated X_n^{m-} species in order to ascertain the correctness of the resulting qualitative conclusions and to get a sound numerical indication of the energies involved.

Computational Details

All of the qualitative aspects discussed in this paper are based on calculations of the extended-Hückel type,[10] using the weighted H_{ij} formula[11] with parameters shown in Table I. Parameters for Fe and W were taken from previous work.[12] Exponents for the Slater orbitals of Br, K, and Cs were taken from Clementi's tables,[13,14] and their orbital energies were taken from ref 15 (Br and K) and ref 16 (Cs).

Quantitative results for Br_4^{n-} and Br_4K_2 species have been computed at the SCF level by using pseudopotentials for the core elements of the Fock matrix as determined from extended all-electron atomic SCF calculations[17] with the help of a modified version[18] of the HONDO program.[19]

The basis set used in the pseudopotential ab initio calculations is of double-ζ quality, with an extra diffuse s function added in order to properly account for the negative charge of the anions[20] and a polarization d function. For a test of the quality of these calculations as compared with full ab initio methods in this family of molecules, see ref 21.

Electronic Structure of X_4 Species[22]

A convenient way to describe the molecular orbitals of a neutral X_4 species is that of two interacting X_2 molecules. From the well-known electronic structure of these diatomic molecules, let us stress the existence of a possible acceptor orbital ($2\sigma^*$) and several potential donor orbitals (mainly 2σ, π, and π^*). If the donor orbital responsible for the formation of a dimer $(X_2)_2$ is

Table I. Orbital Exponents (Contraction Coefficients of Double-ζ Expansion Given in Parentheses) and Energies Used in the Extended-Hückel Calculations

atom	orbital	ζ_μ (c_μ)	ζ_μ' (c_μ')	$H_{\mu\mu}$, eV
Br	4s	2.588		−22.07
	4p	2.131		−13.10
K	4s	0.874		−4.34
	4p	0.874		−2.73
Cs	6s	1.06		−3.88
	6p	1.06		−2.49
Fe	4s	1.90		−9.10
	4p	1.90		−5.32
	3d	5.35 (0.5505)	2.00 (0.6260)	−12.6
W	6s	2.341		−8.26
	6p	2.309		−5.17
	5d	4.982 (0.6940)	2.068 (0.5631)	−10.37

† Departament de Química Inorgànica.
‡ Departament de Química Física.

(1) (a) Coppens, P. In *Extended Linear Chain Compounds*; Miller, J. S., Ed.; Plenum: New York, 1984; Vol. 1, p 333. (b) Marks, T. J.; Kalina, D. W. In *Extended Linear Chain Compounds*; Miller, J. S., Ed.; Plenum: New York, 1984; Vol. 1, p 197.
(2) (a) Tamres, M.; Duerksen, W. K.; Goodenow, J. M. *J. Phys. Chem.* **1968**, *72*, 966. (b) Paschier, A. A.; Christian, J. D.; Gregory, N. W. *J. Phys. Chem.* **1967**, *71*, 937. (c) Paschier, A. A.; Gregory, N. W. *J. Phys. Chem.* **1968**, *72*, 2697. (d) Chance, K. V.; Bowen, K. H.; Winn, J. S.; Klemperer, W. *J. Chem. Phys.* **1980**, *72*, 791.
(3) Shida, T.; Takahashi, Y.; Hatano, H.; Imamura, M. *Chem. Phys. Lett.* **1975**, *33*, 491.
(4) Havinga, E. E.; Boswijk, K. H.; Wiebenga, E. H. *Acta Crystallogr.* **1954**, *7*, 487.
(5) Siepmann, R.; Schnering, H. G. von *Z. Anorg. Allg. Chem.* **1968**, *357*, 289.
(6) Dubler, E.; Linowsky, L. *Helv. Chim. Acta* **1975**, *58*, 2604.
(7) Millan, A.; Bailey, P. M.; Maitlis, P. M. *J. Chem. Soc., Dalton Trans.* **1982**, 73.
(8) Buse, K. D.; Keller, H. J.; Pritzkow, H. *Inorg. Chem.* **1977**, *16*, 1072.
(9) (a) Stoeger, W.; Rabenau, A. *Z. Naturforsch., B: Anorg. Chem., Org. Chem.* **1978**, *33B*, 740. (b) Stoeger, W.; Schulz, H.; Rabenau, A. *Z. Anorg. Allg. Chem.* **1977**, *432*, 5.
(10) Hoffmann, R.; Lipscomb, W. N. *J. Chem. Phys.* **1962**, *36*, 2179, 3489. Hoffmann, R. *J. Chem. Phys.* **1963**, *39*, 1397.
(11) Ammeter, J.; Bürgi, H.-B.; Thibeault, J.; Hoffmann, R. *J. Am. Chem. Soc.* **1978**, *100*, 3686.
(12) Summerville, R. H.; Hoffmann, R. *J. Am. Chem. Soc.* **1976**, *98*, 7240. Dedieu, A.; Albright, T. A.; Hoffmann, R. *J. Am. Chem. Soc.* **1979**, *101*, 3141.
(13) Clementi, E.; Raimondi, D. L.; Reinhardt, W. P. *J. Chem. Phys.* **1967**, *47*, 1300. Clementi, E.; Raimondi, D. L. *J. Chem. Phys.* **1963**, *38*, 2686. Clementi, E.; Roetti, C. *At. Data Nucl. Data Tables* **1974**, *14*, 177.

0002-7863/87/1509-6586$01.50/0

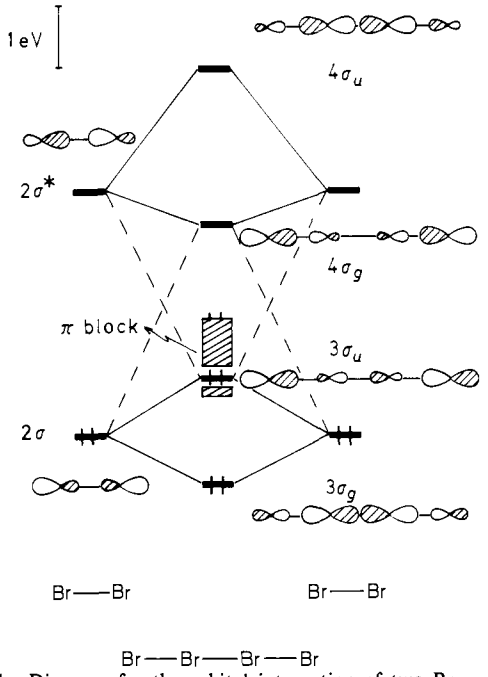

Figure 1. Diagram for the orbital interaction of two Br_2 molecules.

2σ, the expected geometry should be linear and symmetric, while a side-on interaction would be favored if the π orbitals are to act as donors (**1**). An intermediate geometry would combine both 2σ, π, and π^* orbitals as donors.

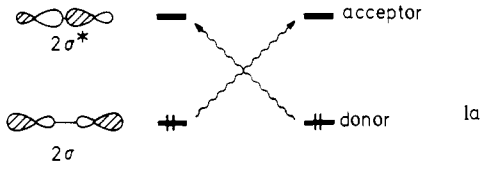

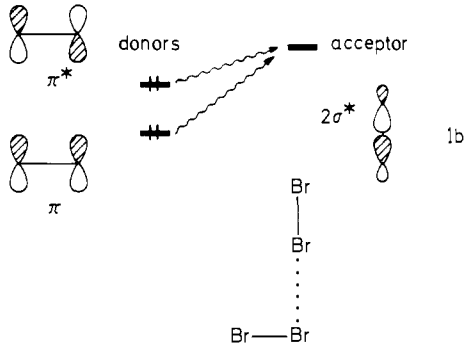

Let us consider the most symmetrical situation first. The essential feature of the σ interactions (Figure 1) is that one bonding orbital ($3\sigma_g$) and one antibonding orbital ($3\sigma_u$) are formed between the X_2 fragments; both are occupied, but mixing of $3\sigma_g$ with $4\sigma_g$ (the bonding combination of the σ^* orbitals of X_2) and of $3\sigma_u$ with $4\sigma_u$ makes them more bonding and less antibonding, respectively, resulting in a net bond formation. This second-order mixing is the MO version of the donor–acceptor approach given in **1**. A fragment population analysis shows that the 2σ orbitals of X_2 are partially depopulated upon dimerization (occupation in Br_4 is 1.88 e) while the $2\sigma^*$ ones are partially populated (0.13 e). A further consequence of these population changes is a weakening of the terminal Br–Br bonds relative to those in their parent molecules: the terminal Br–Br overlap population drops from 0.310 to 0.269. All of these observations are in agreement with the experimental finding of some degree of self-association of the X_2 molecules.[2]

By looking at the topology of the occupied σ molecular orbitals in Figure 1, one can expect the terminal bonds to be stronger than the central one. Indeed, the overlap populations computed by using the same distance for all bonds are 0.269 and 0.106 for the terminal and central bonds, respectively.

On the other hand, the fact that the HOMO–LUMO gap is not large ($\simeq$1.6 eV) may be indicative of a second-order Jahn–Teller instability. The distortions which preserve at least a plane of symmetry are sketched in **2**. The C_{2v} distortion preserves the

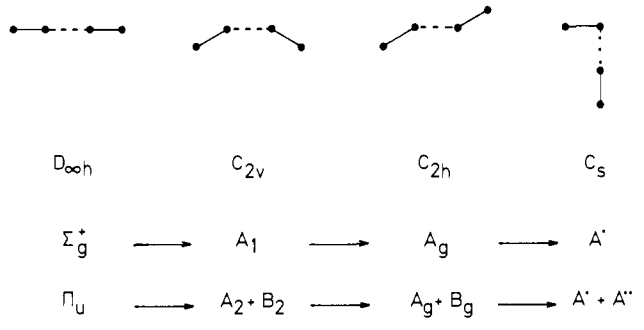

2

σ_h plane of the linear molecule, making the HOMO–LUMO mixing forbidden; consequently, this distortion is not stabilizing. Both C_{2h} and C_s distortions destroy that element of symmetry and thus stabilize the molecule. SCF MO calculations have previously found the C_s structure to be more stable,[23] in agreement with the polar character experimentally found for these molecules[2d] and with the side-on intermolecular contacts found in $(Te_2)_2I_2$ and in the solid halogens and interhalogens Cl_2, Br_2, I_2, ICl, and IBr.[24,25]

We will not go through the details of these distortions here, but let us point out an important detail for the subsequent discussion: the π and π^* orbitals of Br_2 are both occupied, resulting in two-orbital, four-electron repulsions; partial depopulation of π^* should therefore result in enhanced stability. In Br_4 this can be achieved through the donor–acceptor interaction outlined in **1b** for the L-shaped compound.

If an additional electron is placed in $4\sigma_g$ (Figure 1), as in the Br_4^- species, one would expect the external bonds to be weakened whereas the central bond should be slightly strengthened. This is what is actually found in our calculations. This ion is stable against dissociation into Br_3^- and Br•, as reflected in the existence of a minimum in the SCF energy surface at bonding distances.[22] Let us point out, however, that the computed pseudopotential SCF binding energy is negative (−6.3 kcal/mol). This is an artifact of the SCF method since a positive binding energy is found when

(14) Fitzpatrick and Murphy have recently reported an extensive set of parameters for Slater orbitals (Fitzpatrick, N.; Murphy, G. H. *Inorg. Chim. Acta* **1984**, *87*, 41; *Inorg. Chim. Acta* **1986**, *111*, 139) which give a better fit with numerical Hartree–Fock orbitals at short distances, but the electron density at long distances appears to be best reproduced by the usual EH parameters (Wheeler, R.; Hoffmann, R., personal communication).
(15) Hinze, J.; Jaffé, H. H. *J. Chem. Phys.* **1963**, *67*, 1501.
(16) Charkin, O. P. *Russ. J. Inorg. Chem. (Engl. Transl.)* **1974**, *19*, 1590.
(17) Durand, Ph.; Barthelat, J. C. *Theor. Chim. Acta (Berlin)* **1975**, *38*, 283. Pelissier, M.; Durand, Ph. *Theor. Chim. Acta (Berlin)* **1980**, *55*, 43.
(18) Pseudopotentials adaptation by J. P. Daudey, Universite Paul Sabatier, Toulose, France.
(19) Dupuis, M.; Rys, J.; King, H. F. *QCPE* **1977**, *11*, 338.
(20) Chandrasekhar, J.; Andrade, J. G.; Schleyer, P. v. R. *J. Am. Chem. Soc.* **1981**, *103*, 5609.
(21) Novoa, J. J.; Mota, F.; Alvarez, S., submitted for publication.
(22) Part of the results on X_4^- and X_4^{2-} have been reported in a preliminary communication: Alvarez, S.; Novoa, J. J.; Mota, F. *Chem. Phys. Lett.* **1986**, *132*, 531.
(23) (a) Umeyama, H.; Morokuma, K.; Yamabe, S. *J. Am. Chem. Soc.* **1977**, *99*, 330. (b) Prissette, J.; Kochanski, E. *J. Am. Chem. Soc.* **1977**, *99*, 7352. (c) Marsden, C. J. *J. Chem. Soc., Chem. Commun.* **1985**, 786. (d) Kochanski, E. *J. Chem. Phys.* **1982**, *77*, 2691.
(24) Kniepp, R.; Beister, H.-J. *Angew. Chem., Int. Ed. Engl.* **1985**, *24*, 393.
(25) Wells, A. F. *Structural Inorganic Chemistry*, 5th ed.; Oxford University Press: Oxford, 1984.

Table II. Interatomic Overlap Populations and Atomic Charges for Br_2, Linear Br_4, and Linear Br_4^{2-} Computed with All Bond Distances Equal to 2.80 Å

	overlap population		atomic charge	
	terminal	central	terminal	central
Br_2	0.310	0	0	0
Br_4	0.269	0.101	−0.13	0.13
Br_4^{2-}	0.006	0.195	−0.77	−0.23

the electronic correlation is taken into account using an MP2 formalism[26] on the SCF reference function (10.8 kcal/mol). The same behavior of the SCF binding energies has been previously reported for the F_2 molecule[27] and will not be further discussed here. The second-order Jahn–Teller effect is no longer effective, and this species is found to be more stable with a linear than with an angular geometry at the SCF computational level.

X_4^{2-} Species and Their Interaction with Alkaline Ions

The addition of two electrons to an X_4 species has important effects on its structure and stability. Let us worry first about the molecular structure. The HOMO–LUMO gap ($4\sigma_g$–$4\sigma_u$) is much larger now (≃2.6 eV), the driving force for the distortion is largely diminished, and the linear structure is a likely one. Secondly, occupation of $4\sigma_g$ weakens the terminal bonds and strengthens the central one (Table II), reversing the trend found for the neutral species. Roughly speaking, we could say that Br_4 consists of two weakly interacting Br_2 molecules, while Br_4^{2-} consists of a Br_2 molecule weakly bound to two Br^- ions (**3**), as seen in the atomic

$$Br—Br\cdots Br—Br \xrightarrow{2e^-} Br^-\cdots Br—Br\cdots Br^- \qquad 3$$

overlap populations (Table II). Our ab initio calculations on a linear isolated Br_4^{2-} ion with an imposed inversion center gives equilibrium bond distances of 2.48 and 3.48 Å for the central and terminal bonds, respectively, thus confirming its description as $Br_2 + 2\ Br^-$.

Occupation of the $4\sigma_g$ orbital, however, makes the system unstable toward dissociation into Br_3^- and Br^-, as found in our pseudopotential ab initio calculations. We urgently need a Lewis acid to withdraw electron density from the antibonding occupied orbitals and stabilize the Br_4^{2-} ion. Let us examine how an alkali metal cation or a transition-metal fragment does the job.

The interaction of Br_4^{2-} with two alkali metal ions, preserving an inversion center, stabilizes the anion, but the total energy depends on the relative position of the anion and the cations. The potential energies for the potassium and cesium composites, calculated with the extended-Hückel (EH) method, are shown in Figure 2. A side-on geometry is favored over the end-on interaction, a minimum appearing for the location of the alkaline cations close to the terminal Br atom. Since the EH method does not account for internuclear repulsions, calculations at shorter h distances than those included in Figure 2 would be physically unrealistic. What is important is that the number and position of the minima in the potential energy curves does not depend on the value chosen for h.

Ab initio calculations are best suited to evaluate bond distances, and they definitively rule out h values shorter than 2.0 Å for the studied case. Interestingly, the ab initio results are qualitatively consistent with the EH ones: the estimated global minimum (total energy −52.568786 au) corresponds to a side-on geometry with the potassium ions close to the terminal Br atoms (z = 1.03 Å, h = 2.82 Å, α = 110°). The geometry at the minimum presents bond distances $(Br–Br)_{term}$ = 3.48 Å, $(Br–Br)_{central}$ = 2.25 Å, and $K–Br_{term}$ = 3.00 Å. The end-on geometry is some 5 kcal/mol

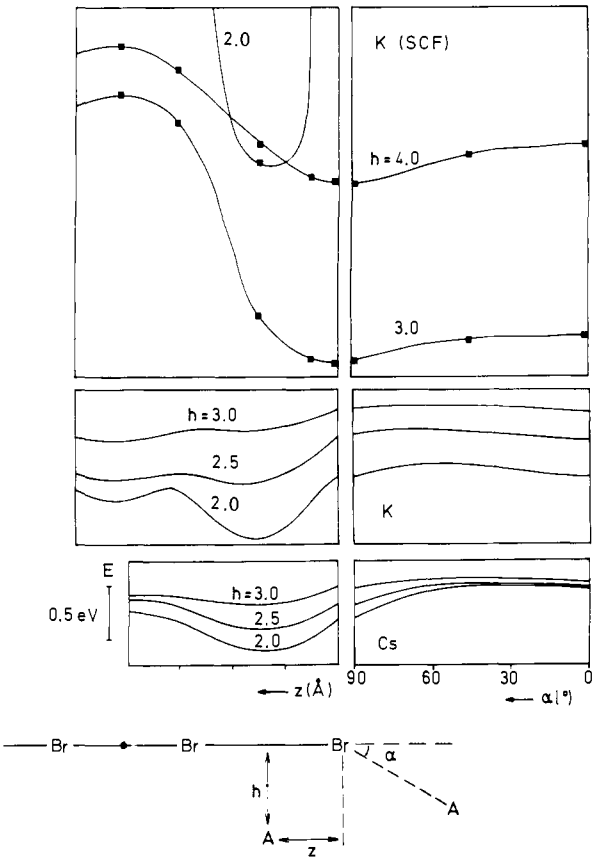

Figure 2. Potential energy curves for the interaction of two alkali metal ions with a Br_4^{2-} group preserving an inversion center. The portions at the left correspond to a displacement of the cations parallel to the Br_4^{2-} group at a fixed distance h, while the right portions correspond to a rotation of the cations around the terminal Br atoms at a fixed $K–Br_{term}$ distance h. The upper curve has been calculated at the pseudopotential ab initio level, and the lower curves have been calculated at the extended-Hückel level.

higher than the side-on one for h = 3.0 Å. A further coincidence of the ab initio and EH results is the existence of a local minimum perpendicular to the center of the Br_4 group for h = 2.0 Å (this part of the curve falls outside the energy window shown in Figure 2 for the SCF case).

The reason for the side-on preference is schematically shown in **4** and **5**: For the end-on geometry, the $3\sigma_u$ and $4\sigma_g$ orbitals can act as donors toward an sp_z acceptor orbital of the alkali metal

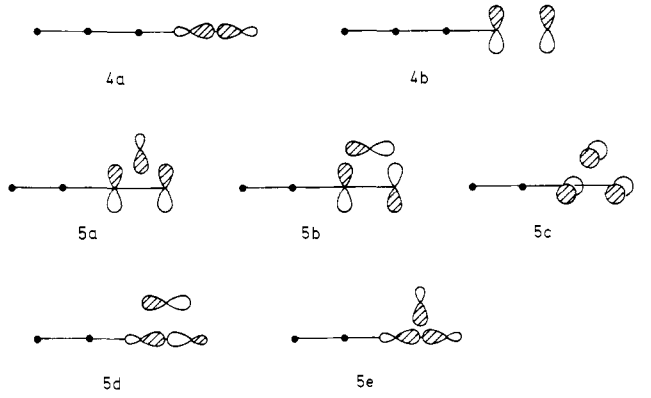

cation (**4a**), and a π-type donation toward the p_x and p_y empty orbitals also exists (**4b**). For the side-on geometry, an sp_x hybrid of the alkali metal ion interacts in a σ way with the $1\pi_u$ and $1\pi_g$ orbitals of X_4^{2-}, and p_y interacts with both $2\pi_u$ and $2\pi_g$ in the same π fashion as for the end-on case (**5c**), but the p_x interaction (**5b**) has now some σ character and is therefore stronger than **4b** for the linear case. Furthermore, σ-type orbitals of Br_4^{2-} can interact

(26) Moller, C.; Plesset, M. S. *Phys. Rev.* **1934**, *46*, 618.
(27) (a) Das, G.; Wahl, A. C. *J. Chem. Phys.* **1966**, *44*, 87. (b) Das, G.; Wahl, A. C. *Phys. Rev. Lett.* **1970**, *24*, 440. (c) Das, G.; Wahl, A. C. *J. Chem. Phys.* **1972**, *56*, 3532. (d) Berkowitz, J.; Wahl, A. C. *Adv. Fluorine Chem.* **1973**, *7*, 147. (e) Kasseckert, E. *Z. Naturforsch., A: Phys., Phys. Chem., Kosmophys.* **1973**, *28A*, 704. (f) Ahlrichs, R.; Lischka, H.; Zurawski, B.; Kutzelnigg, W. *J. Chem. Phys.* **1975**, *63*, 4685. (g) Rescigno, T. N.; Bender, C. F. *J. Phys. B* **1976**, *9*, L329.

Table III. Calculated Overlap Populations and Experimental Bond Distances for X_4^{2-} Ions in the Presence of Cations A

	X_1–X_2	X_2–X_3	X_1–A	X_2–A
	Overlap Populations			
Br_4^{2-}	−0.024	0.384		
Cs_2Br_4	−0.026	0.386	0.128	0.137
	Experimental Bond Distances (Å)			
$Tl_2Ag_6I_{10}$[a]	3.32	2.90	3.60	3.82

[a] Reference 9a.

with the empty orbitals of the cation (**5d**, **5e**). As a result of this geometrical preference, these X_4^{2-} species are well suited to form linear arrays of discrete ions, laterally interacting with the walls of cationic channels.

This stabilizing interaction is highly ionic, as reflected in the small amount of charge transfer from the occupied σ^* and π^* orbitals of Br_4^{2-} to the cations: the net calculated (EH) charge transfer to each K^+ ion is 0.16 e for a terminal Br–K distance of 2.8 Å and is practically independent of the position of the cation ($0 < \alpha < 90°$); a similar result is obtained (EH) for cesium (charge transfer is 0.12 e at 3.0 Å), whereas a net charge transfer of 0.18 e is calculated for potassium using pseudopotential ab initio calculations. Consequently, the Br–Br bonds are only slightly strengthened, and Br_4^{2-} should still look more like a Br_2 molecule weakly interacting with two Br^- ions. This orbital analysis fits nicely with the experimental structures of the known X_4^{2-} species (Table III).

Although one may think that EH calculations greatly underestimate ionic interactions, comparison of the present EH and ab initio results allows us to conclude that these ionic interactions are well described by such a one-electron MO model.

Coordination of Br_4 to a Transition Metal

The general aspects of the bonding of a Lewis base to a transition metal are well-known.[28] We will center our attention on two main aspects of the coordination of Br_4 and Br_4^{2-}: their preferential coordination modes and their stabilization upon coordination.

If Br_4 is to act as a bridging ligand, two donor orbitals are necessary, a symmetric and an antisymmetric combination. Two such σ-type orbitals are available for a linear coordination **6**: $3\sigma_g$ and $3\sigma_u$. An alternative bridging mode is **7**, with right M–Br–Br

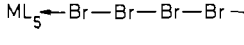

6

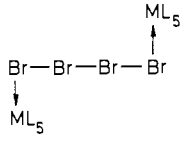

7

angles; the bonding for different M–Br–Br angles can be understood in terms of these two extreme cases. In **7**, the π and π^* orbitals of Br_4 or Br_4^{2-} can act as donors, and their energies and topologies are best suited to interact with the symmetry-adapted combinations of the metal acceptor orbitals.

Let us consider the most symmetric case first, the linear structure **6** with D_{4h} symmetry (the fourfold axis is coincident with the M–Br_4–M bond sequence). A diagram for the interaction of Br_4 with a d^6-ML_5 group is presented in Figure 3. The highest four orbitals shown are essentially the e_g sets of the two metal atoms. At lower energies appear several orbitals of the Br_4 group interspersed with the t_{2g} sets of both metal atoms (the d_{xy} orbitals are not shown). Four of these molecular orbitals are of σ type, two bonding ($1a_{1u}$ and $1a_{1g}$) and two antibonding ($2a_{1u}$ and $2a_{1g}$). The centrosymmetric molecular orbitals are formed as combinations of $4\sigma_u(Br_4)$ and $(d_{z^2})^+$ (the in-phase combination of both

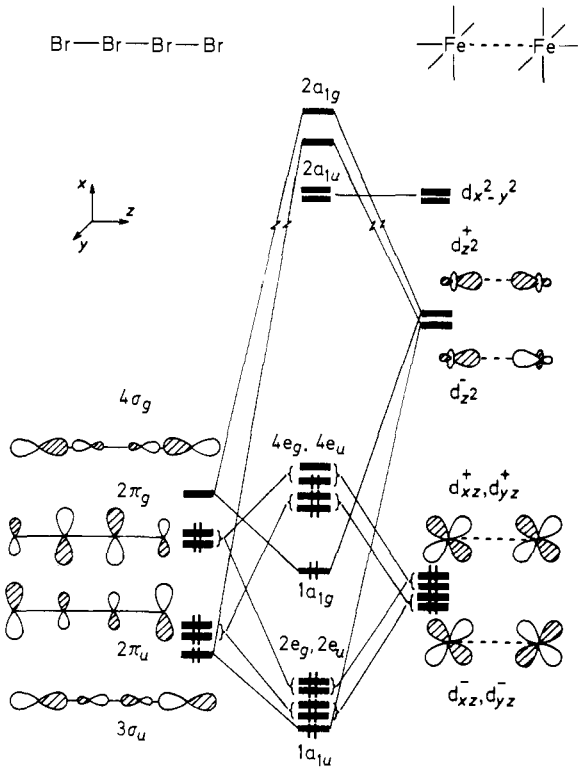

Figure 3. Diagram for the orbital interaction of two d^6-ML_5 fragments with a bridging Br_4 group. The $d_{z^2}^+$ and $d_{z^2}^-$ orbitals of the Fe_2L_{10} fragment are essentially degenerate because of the long Fe–Fe distance.

d_{z^2} orbitals); they were initially empty orbitals in the isolated Br_4 and ML_5 fragments, but their bonding combination is now occupied. As a consequence, one of the π ($4e_g$) orbitals (mainly d_{xz}, metal–ligand antibonding) is emptied, resulting in a formal reduction of Br_4 to Br_4^{2-} and a formal oxidation of the d^6 metals to d^5.

The fact that $4\sigma_g$ is stabilized through interaction with $d_{z^2}^+$ has an important structural consequence: the mixing of $4\sigma_g$ with $2\pi_u$ (identified in the complex as the $4e_u$ and $1a_{1g}$ occupied orbitals) does not produce any stabilization now, and the driving force for the distortion of Br_4 toward an L shape found in the free ligand is lost. Hence, the coordinated Br_4 is more stable in its linear conformation.

The partial occupation of the $4e_g$ degenerate set, on the other hand, produces a Jahn–Teller instability. The stabilizing distortion in this case is the angular deformation of the M–Br_4–M skeleton (**6** → **7**). The calculated total energy curve for such a distortion is shown in Figure 4 (upper part), where a clear preference for an angular structure can be appreciated, regardless of the Br–Br distances used for our calculations, the minimum appearing at $\alpha \simeq 110°$. This distortion can be best understood at the orbital level with the help of a Walsh diagram, shown in Figure 5, where the molecule is kept in the xz plane.

All of the π orbitals form degenerate pairs in the linear molecule; upon angular distortion the e sets are split: the π_y orbitals remain unchanged but the π_x ones are largely affected. The largest variations appear in the energy of one of the $4e_g$ orbitals, essentially d_{xz}^+ (the symmetric combination of the metals' d_{xz} orbitals), mixing in some $2\pi_g(Br_4)$ contribution in an antibonding way. The overlap between these two fragment orbitals is progressively lost with increasing α, as can be seen in the rising energy of its bonding counterpart, one of the $3e_g$ orbitals. However, in the angular situation, d_{xz}^- starts to overlap with $1a_{1g}$ (which can be approximately described as $4\sigma_g$ of Br_4), becoming an antibonding π-type orbital at $\alpha = 90°$. The overlap reaches a maximum at a larger angle because of the interaction with the inner Br atom at $\alpha \simeq 90°$.

For Br_4 and d^6-ML_5, the HOMO is one of the $4e_g$ pair of orbitals, and the minimum at $\alpha \simeq 110°$ can be undoubtedly

(28) (a) Albright, T. A. *Tetrahedron* **1982**, *38*, 1339. (b) Albright, T. A.; Burdett, J. K.; Whangbo, M.-H. *Orbital Interactions in Chemistry*; Wiley: New York, 1985.

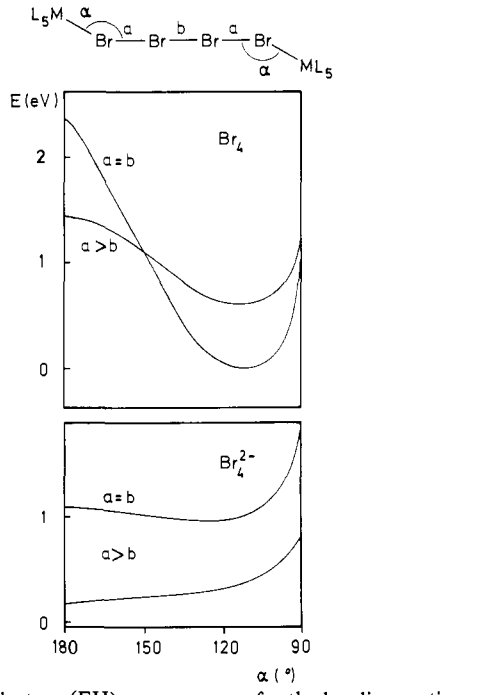

Figure 4. One-electron (EH) energy curves for the bending motion of a $(\mu\text{-}Br_4^{n-})(FeH_5^{3-})_2$ dinuclear complex. The two curves shown correspond to a Br_4 group with all distances equal to 2.80 Å ($a = b$), and with distances of 2.98 Å (terminal bonds) and 2.43 Å (central bond) ($a > b$ curve).

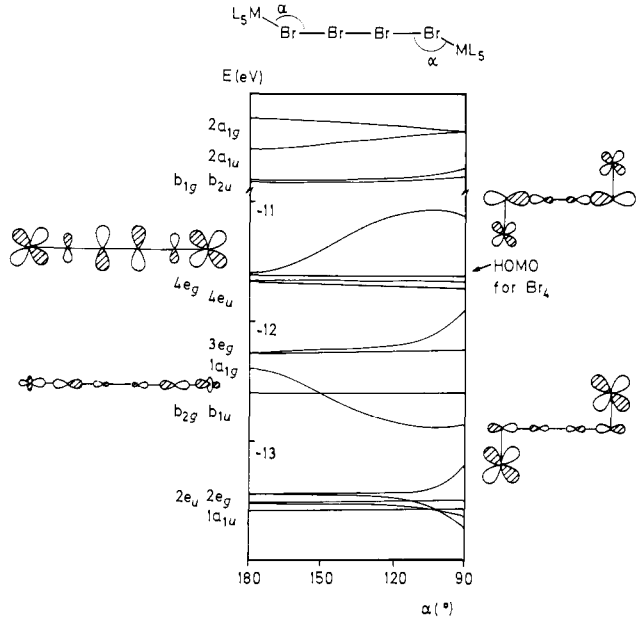

Figure 5. Walsh diagram for the angular distortion of $(\mu\text{-}Br_4)(FeH_5^{3-})_2$ with experimental Br–Br bond distances as in Figure 4 ($a > b$).

attributed to the stabilization of $1a_{1g}$, i.e., to the better π bonding of d_{xz} with $4\sigma_g$ than with $2\pi_g$. This difference can, in turn, be attributed to the different localization of these orbitals: $2\pi_g$ is mostly localized on the central Br atoms whereas $4\sigma_g$ is mainly localized on the terminal ones (the shape of this orbital is represented in Figure 1).

What happens to the Fe–Br σ bond along this distortion? It is kept fairly constant, as can be seen from the energies of the σ-antibonding orbitals $2a_{1u}$ and $2a_{1g}$; only donation to $d_{x^2-y^2}$ (the empty lobe of ML_5) comes now from the $1\pi_g$ and $2\pi_u$ orbitals of Br_4.

Sudden changes in the energies of other orbitals at small angles reflect the onset of interactions of other ligands and of the d orbitals with the inner Br atoms. These interactions are two-orbital, four-electron ones, the usual way in which EH represents the steric repulsions. Steric repulsions are therefore responsible for the rise in energy at low angles in the total energy curve (Figure 4).

Table IV. Calculated Overlap Populations and Experimental Bond Distances in X_4^{2-} Species ($n = 0, 2$)[a]

species	compd	X–X bond dist, Å (overlap pop) central	terminal	ref
X_4	$(FeH_5^{3-})_2Br_4$ ($\alpha = 110°$)	(0.335)	(0.093)	
	W_6Br_{16}	2.43	2.98, 2.98	5
X_4^{2-}	Br_4^{2-}	(0.384)	(−0.024)	
	$(FeH_5^{3-})_2Br_4^{2-}$	(0.398)	(−0.017)	
	$Pt(phen)I_5$	2.739	3.289, 3.457	8
	$Pt(phen)I_6$	2.750	3.452, 3.481	8
	$Ir_2Cp_2I_6$	2.750	3.241, 3.557	7
	$Cu(NH_3)_4I_4$	2.802	3.342, 3.342	6

[a] The experimental Br–Br distances in W_6Br_{16} have been used in EH calculations.

In summary, the bonding between Br_4 and d^6-ML_5 in the angular situation can be described as a four-electron donation from the π orbitals of Br_4 to the $d_{x^2-y^2}$ orbitals of the metals (each $d_{x^2-y^2}$ orbital is populated by 0.5 e after interaction with Br_4), plus a back-donation from d_{xz} to the σ LUMO of Br_4 ($4\sigma_g$, occupied by 0.6 e). One could also expect back-donation from d_{xz}, the out-of-phase combination of the d_{xz} orbitals, but the only empty orbital with the appropriate symmetry in Br_4 is $4\sigma_u$, too high in energy and centered on the central Br atoms, resulting in a donation of less than 0.01 e).

The only transition-metal derivative of X_4 known so far is W_6Br_{16},[5] which can be best described as $\{(W_6Br_{12})(\mu\text{-}Br_4)\}_\infty$, an octahedral cluster of tungsten atoms with bridging Br_4 groups axially coordinating to two tungstens in trans vertices of the octahedron. The usual electron-counting rules for clusters,[29] as well as our EH calculations on the W_6Br_{12} fragment,[30] indicate that it must be considered as a neutral fragment coordinating two two-electron donors at both apical positions. Hence, the description of the cluster as a Br_4^0 bridging two d^6-ML_5 fragments correctly represents the bonding. Although the calculated angle ($\alpha \simeq 110°$) should depend on the set of ligands present in the transition-metal fragment, it is encouraging to verify that the experimental angle is 111°.

The overlap population for the central Br–Br bond is larger than that for the terminal bonds (0.335 and 0.093, respectively), and the Br–Br bond distances found in W_6Br_{16} agree well with this difference in overlap populations: the central bond is close to that in Br_2 in the solid state (2.27 Å) and the terminal ones are longer than in Br_2 but clearly shorter than the intermolecular contacts of 3.31 Å.[31]

According to the Walsh diagram (Figure 5), the ground state for the linear geometry ($\alpha = 180°$) would be a triplet. The problem of evaluating the relative stability of the triplet linear structure against the singlet bent form cannot be handled by EH calculations, where two-electron terms are neglected. However, as the weight of one-electron terms in the total energy of ab initio computations is usually much higher than that of the two-electron terms, one can expect that the stabilization upon bending of the $1a_{1g}$ orbital present in the singlet state would be higher than the stabilization of the linear triplet caused by exchange contributions.

Coordination of Br_4^{2-} to a Transition Metal

According to the interaction diagram (Figure 4), coordination of Br_4^{2-} to a d^6-ML_5 fragment would fill all the molecular orbitals

(29) (a) Wade, K. In Johnson, B. F. G., ed. *Transition Metal Clusters*; Wiley: New York, 1980; p 193. (b) Wade, K. *Adv. Inorg. Chem. Radiochem.* **1976**, *18*, 1. (c) Rudolph, R. W. *Acc. Chem. Res.* **1976**, *9*, 446. (d) Grimes, R. N. *Acc. Chem. Res.* **1978**, *11*, 420. (e) Lauher, J. W. *J. Organomet. Chem.* **1981**, *213*, 25.

(30) For a description of the molecular orbitals of octahedral M_6L_n clusters, see: Halet, J.-F.; Hoffmann, R.; Saillard, J.-Y. *Inorg. Chem.* **1985**, *24*, 1695. Woolley, R. G. *Inorg. Chem.* **1985**, *24*, 3519.

(31) Donohue, J.; Goodman, S. H. *Acta Crystallogr.* **1965**, *18*, 568.

up to $4e_g$. The major effect of the coordination on Br_4^{2-} is the partial depopulation of the σ-antibonding orbitals $3\sigma_u$ and the HOMO $4\sigma_g$ (occupations in the linear model complex are 1.60 and 1.61 e, respectively), therefore stabilizing the Br_4^{2-} ligand, as can be seen in the Br–Br overlap populations (Table IV). Comparison of the extent of electron transfer to a transition metal with that in the alkali metal cation composite discussed above, clearly shows that the transition metal is more efficient in stabilizing the unstable Br_4^{2-} species.

Again, the atomic overlap populations suggest a strong central but a very weak terminal Br–Br bond. Unfortunately, no complexes of Br_4^{2-} are known so far, but this trend is obvious in the bond distances of I_4^{2-} complexes presented in Table IV. These bond distances can be compared to 2.667 and 2.72 Å in I_2 in the solid and in the gas phase[25,32] and to the intermolecular contacts of 3.50 and 3.324 Å in I_2 and $(Te_2)_2I_2$ in the solid state.[24,29,33] All of these data point to a description of the X_4^{2-} species as a central X_2 weakly interacting with two bromide ions. The calculated atomic charges for the central and terminal Br atoms are 0.0 and −0.4, respectively, at the EH computational level. The calculated charge transfer from the Br_4^{2-} ion to the transition-metal fragments is therefore 1.2 e, much larger than that found above for alkali metal cations (0.1–0.2 e), indicating that transition-metal fragments are much more efficient in stabilizing the X_4^{2-} groups than the alkali metal cations.

There is still something puzzling in the I_4^{2-} structures: despite the large HOMO–LUMO gap, the known compounds are not linear. A calculation on our model compound with the experimental distances for Br_4 gives a minimum for the linear molecule, but the energy curve is almost flat (Figure 4). If we let all the Br–Br bond distances be the same, a minimum is found for $\alpha \simeq 120°$. In any case, the energy difference between both structures is rather small and it is controlled by the interactions between the d_{xz} orbitals of the metal and the occupied orbitals of Br_4^{2-}, formally, four-electron repulsions.

In view of the above results we must conclude that X_4^{2-} species should in general be expected to be stable as ligands in transition-metal complexes, and the scarcity of well-characterized examples is only due to the lack of synthetic attempts.

Acknowledgment. We are indebted to CAICYT for financial support (Grant No. 0657/81).

Registry No. Br_4, 12595-73-2; Br_4^{2-}, 12595-74-3; Br_2, 7726-95-6; K^+, 24203-36-9; Cs^+, 18459-37-5.

(32) Vilkov, L. V.; Mastryukov, V. S.; Sadova, N. I. *Determination of the Geometrical Structure of Free Molecules*; Mir: Moscow, 1983.
(33) Koster, P. B.; Migchelsen, T. *Acta Crystallogr.* **1967**, *23*, 90.

Origin of Methyl Conformational Preferences and Rotational Barriers in the Ground States, Excited Triplet States, Radical Cations, and Radical Anions of Molecules Having CH_3–C=X Functionalities

Andrea E. Dorigo,[†] David W. Pratt,*[‡] and K. N. Houk*[†]

Contribution from the Department of Chemistry and Biochemistry, University of California, Los Angeles, California 90024, and Department of Chemistry, University of Pittsburgh, Pittsburgh, Pennsylvania 15260. *Received January 15, 1987*

Abstract: Ab initio molecular orbital calculations have been carried out on the ground states, triplet states, radical cations, and radical anions of propene, acetaldehyde, acetaldehyde imine, dimethylbutadiene, and biacetyl. The barrier to methyl group rotation was calculated in each case by geometry optimization with the 3-21G basis set, and, for several cases, subsequent energy calculations were performed with the 6-31G* basis set with inclusion of MP2 correlation energy corrections. It is shown that the conformation about the C(methyl)–C(=X) bond is determined by the relative importance of the repulsion between filled orbitals, which favors "eclipsed" conformations for the ground states (as in ethane), and the overlap between vacant and filled orbitals, which favors eclipsed conformations for ground states and staggered conformations for excited states, and becomes the dominant effect in excited states.

The ground states of propene,[1] acetaldehyde and simple methyl ketones,[2] and acetaldehyde imine derivatives[3] prefer methyl group conformations that have a C–H bond syn or eclipsed with the double bond (**1**). The same conformational preference is exhibited

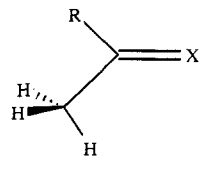

1

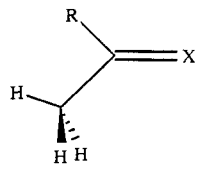

2

in conjugated dienes, such as dimethylbutadiene,[4] and in α-dicarbonyl compounds, such as methylglyoxal.[5] Several theoretical calculations have been published that support and provide explanations of the experimental results for simple olefins, aldehydes, and ketones.[6-9] On the other hand, there have been no systematic

[†] University of California, Los Angeles.
[‡] University of Pittsburgh.

(1) (a) Kilpatrick, J. E.; Pitzer, K. S. *J. Res. Natl. Bur. Stand. (U.S.)* **1946**, *37*, 163. (b) Lide, D. R.; Mann, D. E. *J. Chem. Phys.* **1957**, *27*, 868. (c) Möller, K. D.; DeMeo, A. R.; Smith, D. R.; London, L. H. *Ibid.* **1967**, *47*, 2609.
(2) Acetaldehyde: (a) Kilb, R. W.; Lin, C. C.; Wilson, E. B., Jr. *J. Chem. Phys.* **1957**, *26*, 1695. (b) Herschbach, D. R. *Ibid.* **1959**, *31*, 91. Acetone: Smith, D. R.; McKenna, B. K.; Møller, K. D. *J. Chem. Phys.* **1966**, *45*, 1904.
(3) Meier, J.; Bauer, A.; Günthard, H. H. *J. Chem. Phys.* **1972**, *57*, 1219.
(4) Durig, J. R.; Compton, D. A. C. *J. Phys. Chem.* **1979**, *83*, 2879.
(5) Dyllick-Brenzinger, C. E.; Bauder, A. *Chem. Phys.* **1978**, *30*, 147.
(6) Compounds with threefold barriers: (a) Cremer, D.; Binkley, J. S.; Pople, J. A.; Hehre, W. J. *J. Am. Chem. Soc.* **1974**, *96*, 6900. (b) Bernardi, F.; Bottoni, A.; Tonachini, G. *J. Chem. Soc., Perkin Trans. 2* **1980**, 467. (c) Hehre, W. J.; Pople, J. A.; Devaquet, A. J. P. *J. Am. Chem. Soc.* **1976**, *98*, 664. (d) Pross, A.; Radom, L.; Riggs, N. V. *J. Am. Chem. Soc.* **1980**, *102*, 2253.

0002-7863/87/1509-6591$01.50/0